

Turbulence effects in planetesimal formation

Lindsay S. Hodgson¹ and Axel Brandenburg²

¹ Department of Physics, University of Newcastle upon Tyne, NE1 7RU, UK

² Department of Mathematics, University of Newcastle upon Tyne, NE1 7RU, UK

Received 15 July 1997 / Accepted 27 October 1997

Abstract. The formation of planetesimals is investigated by studying the transport of dust particles in a local three-dimensional simulation of accretion disc turbulence. Heavy particles fall rapidly towards the midplane, whereas lighter particles are strongly advected by the flow. For light particles the turbulence leads to a rapid redistribution of particles such that their density per unit mass is approximately constant with height. There is no pronounced concentration of particles in vortices or anticyclones, as was suggested previously. This is partly because of the adverse effect of keplerian shear and also because in our simulation vortices are only short lived. However, if we assume the gas velocity to be frozen in time, there is a concentration of dust in ring-like structures after a few orbits. This is caused mainly by a convergence of the gas flow in those locations, rather than the presence of vortices or anticyclones.

Key words: solar system: formation – turbulence

1. Introduction

Planetesimals are the progenitors of planets. Once planetesimals have grown to a size of a few ten kilometers their random dispersion velocity is small and planets can form owing to gravitational collapse. Planetesimals are thought to be formed from grains and dust in the gaseous protostellar disc or the solar nebula. Coagulation of grains and small particles could accelerate the settling of particles towards the midplane (Goldreich & Ward 1973). However, turbulence in the gaseous disc would constantly stir up the particles and inhibit particle settling. On the other hand, turbulence also enhances the rate of mutual collisions of particles which would speed up their growth by coagulation (Weidenschilling 1980, 1984 and Weidenschilling & Cuzzi 1993; see also Lin & Papaloizou 1993 for a review).

There came a new twist to the debate when Barge & Sommeria (1995) and Tanga et al. (1996) proposed that dust particles could be trapped within turbulent anticyclonic eddies. It is as yet unclear however, whether turbulent eddies are really in the

form of long-lived vortices. By analogy with Jupiter's Great Red Spot the answer seems to be yes (Abramowicz et al. 1992), but in the presence of a magnetic field vortices may only be short-lived (Dubrulle & Valdetaro 1992), as is also seen in simulations of magnetised accretion disc turbulence (Brandenburg et al. 1995a).

In the present paper we wish to test the idea of particles being trapped in vortices or anticyclones. This investigation is timely, because we are now in a situation where three-dimensional models of accretion disc turbulence are available to study such effects.

Until very recently the origin and nature of turbulence in accretion discs in general has been quite unclear. This is because keplerian accretion discs are stable, so there would be no mechanism that drives the turbulence. Although several solutions have been offered, e.g. nonlinear instability (Dubrulle 1993) or convection (Kley et al. 1993), no simulations have yet been presented that show that such mechanisms actually work and lead to self-sustained turbulence. This is also true for the mean-field calculations of Cuzzi et al. (1993), who considered particle-gas dynamics in a protoplanetary nebula, assuming that turbulence results from vertical shear between the gas and particle layers. Another source of turbulence arises in the presence of a magnetic field, because then any differentially rotating fluid with $d\Omega^2/dR < 0$ is unstable (Balbus & Hawley 1991, 1992). Subsequent three-dimensional calculations have shown that this instability does indeed lead to turbulence (Hawley et al. 1995, Matsumoto & Tajima 1995, Brandenburg et al. 1995a) and that turbulence can be self-sustained due to dynamo action (Brandenburg et al. 1995a, Hawley et al. 1996, Stone et al. 1996).

In order for magnetic fields to be important in protostellar discs, two criteria have to be satisfied. First of all the magnetic Reynolds number has to be large enough (at least around one hundred), and secondly the coupling between neutrals and ions has to be strong enough. More specifically, the ratio of the neutral-ion collision frequency to the orbital frequency has to exceed unity (Blaes & Balbus 1994, see also Brandenburg et al. 1995). Regös (1997) has estimated that at a distance of 1 AU from the protosun this ratio was in fact around 300. However, the first problem may be more stringent. Stepinski et al. (1993) have estimated that the conductivity is so poor that the magnetic

Reynolds number could well be below one hundred within a belt of around 1 AU around the protosun (see also Reyes-Ruiz & Stepinski 1995). However, magnetic fields will still play a role in all other parts of the disc and at larger heights above the midplane, where cosmic ray ionisation is very efficient.

In the following, we use data of simulations of a model similar to Run B of Brandenburg et al. (1996). With the simulations we try to answer two important questions. How efficient is the stirring up of particles in the vertical direction and how rapidly can particles concentrate in the horizontal direction, possibly into anticyclones. We anticipate that the stirring up of particles in the vertical direction is less efficient than in the other directions because in accretion discs rapid rotation (in the sense of large inverse Rossby numbers) has the tendency to make the turbulence two-dimensional. On the other hand, the flow cannot be strictly two-dimensional, because the turbulence is sustained by dynamo action which requires the flow to have a three-dimensional component. There is yet another possibility that could affect particle accumulation, which can be addressed using turbulence simulations. Elperin et al. (1996) have shown that particles tend to accumulate near a temperature minimum. For example, aerosols would concentrate around the temperature inversion layer in the tropopause of the earth. However, if this effect is present in accretion discs it would probably contribute to driving particles even further away from the midplane.

We begin by discussing the basic equations of particle transport in protostellar discs. We then consider a simple two-dimensional model to investigate the effect of shear on the capture of particles in anticyclones. Finally we use data of the fully three-dimensional simulations to compute particle transport.

2. Particle transport

We assume here that the simultaneous evolution of gas and solid particles in a protoplanetary disc can be described using the 2-fluid equations for the gas component and a solid particle component. The particle phase is described by the velocity \mathbf{u}_p , number density n_p , and the mass of individual particles m_p . The gas phase, on the other hand, is described by the velocity \mathbf{u} , the number density n and the mass of individual gas atoms or molecules m . Their product is the gas density $\rho = nm$.

The physically important effects include gravity, centrifugal and Coriolis forces, pressure gradients, as well as magnetic and viscous forces. In a frame of reference rotating with the angular velocity Ω the equation of motion of the gas takes then the form

$$nm \frac{D\mathbf{u}}{Dt} = -\nabla p + nm(\mathbf{g} - 2\Omega \times \mathbf{u} + 2q\Omega^2 \mathbf{x}) + \mathbf{F} - \beta(\mathbf{u} - \mathbf{u}_p), \quad (1)$$

where $D\mathbf{u}/Dt$ is the Lagrangian time derivative, \mathbf{F} denotes magnetic and viscous forces, $\mathbf{x} = (x, 0, 0)$ and $2q = -d\Omega^2/d \ln R$ results from the balance between radial gravity and the centrifugal force. The coupling between the gas and the particles via collisions is governed by the parameter β . The corresponding equation of motion for the particles is similar,

$$n_p m_p \frac{D\mathbf{u}_p}{Dt} = n_p m_p (\mathbf{g} - 2\Omega \times \mathbf{u}_p + 2q\Omega^2 \mathbf{x}_p) - \beta(\mathbf{u}_p - \mathbf{u}). \quad (2)$$

Here we have assumed, however, that the particles do not experience pressure support nor magnetic or viscous forces. We note here that the effect of brownian motion would lead to particle diffusion. This is crucial for the effects discussed by Elperin et al. (1996) and would need to be included in future work. We also point out that in equations (1) and (2) the coupling constant β is the same, so the coupling preserves the total momentum. Physically, the coupling results from the viscous drag between the solid particles and the surrounding gas. In the laminar regime, and if the mean-free path, ℓ , of the gas particles is short compared with the radius, a_p , of the particles, the coupling is given by Stokes drag. In the absence of a background flow, the drag force F_D acting on a single particle is

$$\mathbf{F}_D = -k\rho c_s \ell a_p \mathbf{u}_p, \quad (3)$$

where k is a numerical coefficient and c_s the speed of sound. (Here we have assumed that the kinematic viscosity is given by $\nu = \frac{1}{3}\ell c_s$.) Stokes drag is only valid when $\ell \ll a_p$. In the opposite case, when $\ell \gg a_p$, i.e. the Epstein regime, we have to replace ℓ by a_p . So, in general we may write

$$\mathbf{F}_D = -k\rho c_s \min(\ell, a_p) a_p \mathbf{u}_p. \quad (4)$$

[For a more precise expression valid in the two regimes see Seinfeld (1986).] It is convenient to introduce the stopping time τ_p of a single particle (in the absence of other forces) via

$$\tau_p^{-1} = \frac{\beta}{n_p m_p}. \quad (5)$$

This stopping time is proportional to the drag force per unit mass, so $\tau_p^{-1} a_p = F_D/m_p$. We express m_p in terms of its volume, $(4\pi/3)a_p^3$, and the density ρ_p of the solid material, so

$$\tau_p^{-1} = \tilde{k} \frac{\rho}{\rho_p} \frac{c_s}{a_p} \min(1, \ell/a_p), \quad (6)$$

where $\tilde{k} = 3k/4\pi$. In the following we assume for simplicity $\tilde{k} = 1$. The quantity $2\Omega\tau_p$ plays an important role in the particles dynamics. If $2\Omega\tau_p > 1$ then viscous drag is relatively unimportant and the particles follow a free fall towards the midplane. For $2\Omega\tau_p < 1$ the particles are strongly coupled to the gas.

In accretion discs the isothermal sound speed c_s is related to the the density scale height H via $c_s = H\Omega$, where H describes the density stratification via $\rho = \rho_0 \exp[-z^2/(2H^2)]$. This allows us to express τ_p in normalised form,

$$2\Omega\tau_p = 2 \frac{\rho_p}{\rho} \frac{a_p}{H}. \quad (7)$$

Typical values for the protosolar nebula are $\rho_p/\rho = 10^{10}$ and $H = 10^{12}$ cm, so a value $2\Omega\tau_p = 2$ corresponds to meter-sized particles, $2\Omega\tau_p = 0.02$ to centimeter-sized particles and $2\Omega\tau_p = 2 \times 10^{-6}$ to micrometer-sized particles.

Before we proceed, let us first discuss the relative importance of the drag term in the two equations for the particles and the gas. The time scale of the drag acting on the

gas is $\tau = \beta/\rho$. The ratio of the two time scales is then $\tau/\tau_p = nm/(n_p m_p) = M/M_p$, where M and M_p are the total masses of gas and particles in the disc. Of course at later times, when the disc is cleared out, this ratio will be much smaller than unity, but at early times the disc is still gas-rich, so $M/M_p \gg 1$. In that case we may neglect the backreaction of the particles on the gas. In the following we shall make this assumption.

3. Preliminary considerations

We consider a local approximation and use a cartesian coordinate system, where x corresponds to the radial direction, y to the azimuthal direction, and z to the vertical direction. For details regarding this approximation see Lynden-Bell & Ostriker (1967), Wisdom & Tremaine (1988), and Balbus (1996). We want to understand those conditions under which particles tend to accumulate and where. We shall identify regions of convergence with those locations where the divergence of the particle velocity is negative.

For the present discussion it is sufficient to consider the linearised momentum equation (2)

$$\frac{\partial \mathbf{u}_p}{\partial t} = \mathbf{g} - 2\boldsymbol{\Omega} \times \mathbf{u}_p + 2q\Omega^2 \mathbf{x}_p - \tau_p^{-1}(\mathbf{u}_p - \mathbf{u}). \quad (8)$$

In thin discs $\mathbf{g} = (0, 0, -\Omega^2 z)$. In the special case $\tau_p^{-1} = 0$, this equation has the steady solution $\mathbf{u}_p = -q\Omega x \hat{\mathbf{y}}$, where $\hat{\mathbf{y}}$ is the unit vector in the y -direction. Following now the approach of Barge & Sommeria (1995) and Tanga et al. (1996) we consider only the two-dimensional case, $\mathbf{u} = (u_x, u_y, 0)$, with $\partial/\partial z = 0$, and $\boldsymbol{\Omega} = (0, 0, \Omega)$. We assume the gas flow to be solenoidal, i.e. $\nabla \cdot \mathbf{u} = 0$. Taking separately the curl and divergence of this equation we obtain a set of two scalar equations for the two unknowns $\nabla \cdot \mathbf{u}_p$ and $2\boldsymbol{\Omega} \cdot \boldsymbol{\omega}_p$, where $\boldsymbol{\omega}_p = \nabla \times \mathbf{u}_p$,

$$\frac{\partial}{\partial t} (2\boldsymbol{\Omega} \cdot \boldsymbol{\omega}_p) = -4\Omega^2 (\nabla \cdot \mathbf{u}_p) - 2\Omega\tau_p^{-1} \cdot (\boldsymbol{\omega}_p - \boldsymbol{\omega}), \quad (9)$$

$$\frac{\partial}{\partial t} (\nabla \cdot \mathbf{u}_p) = 2\boldsymbol{\Omega} \cdot \boldsymbol{\omega}_p + (2q - 1)\Omega^2 - \tau_p^{-1} (\nabla \cdot \mathbf{u}_p). \quad (10)$$

Eliminating $2\boldsymbol{\Omega} \cdot \boldsymbol{\omega}_p$ yields the final equation

$$\left[4\Omega^2 \tau_p^2 + (1 + \tau_p \partial_t)^2 \right] (\nabla \cdot \mathbf{u}_p) = \Omega\tau_p \cdot [2\boldsymbol{\omega} + (2q - 1)\boldsymbol{\Omega}]. \quad (11)$$

From now on we assume keplerian rotation, i.e. $q = 3/2$. In the steady state there will be particle accumulation when the divergence of the particle flow is negative, i.e.

$$2\boldsymbol{\Omega} \cdot (\boldsymbol{\omega} + \boldsymbol{\Omega}) < 0. \quad (12)$$

In the absence of shear, particle accumulation would occur in those places where the vorticity of the gas is opposite to the rotation vector, i.e. in anticyclones. This is in agreement with the conclusions drawn by Tanga et al. (1996). In the presence of shear, however, the vorticity is effectively replaced by the total vorticity, $\boldsymbol{\omega} + \boldsymbol{\Omega}$. This new condition is harder to satisfy, as will be seen below.

4. Particle transport in 3-D simulations

4.1. Frozen velocity field

In reality the flow will be three-dimensional. If the disc is gas rich we may neglect the backreaction of the particles on the flow. In particular, we may use existing data of simulations of turbulence in accretion discs such as those of Brandenburg et al. (1995a, 1996). Unfortunately, snapshots have not been taken frequently enough to allow interpolation between them. Therefore we shall use as a first approximation a single snapshot and advance the particle positions in time using the same flow field for the gas at all later times. This approximation may seem rather crude, but experience with similar work in the past (Brandenburg et al. 1995b, Miesch et al. 1995) suggest that at least statistical properties are almost indistinguishable whether or not the flow field was evolving in time. However, as we shall see below, where we solve the flow equations simultaneously with the particle equations, the assumption of a frozen velocity field is not a good approximation at all as far as the accumulation properties of particles is concerned.

Given the gas velocity \mathbf{u} , we solve Eq. (2) for different values of the parameter $2\Omega\tau_p$. In the absence of turbulence and magnetic fields the gas is stratified like $\rho = \rho_0 \exp(-z^2/2H^2)$, where H is the scale height which is proportional to the temperature. The extent of the computational domain is $|z| \leq L_z \equiv 2H$ in the vertical direction, $|x| < L_x \equiv H/2$ in the radial direction, and $|y| < L_y \equiv \pi H$. The gas simulation is carried out on a mesh with $31 \times 63 \times 63$ mesh points. We use a snapshot taken at time $25.3 T_{\text{rot}}$, where $T_{\text{rot}} = 2\pi/\Omega$ is the rotation period, and $\Omega = \sqrt{GM/R^3}$ is the keplerian velocity and $R = 10H$ is the distance of the box from the central object. For further details see the original paper (Brandenburg et al. 1995a). We use here the same parameters as for Run B of Brandenburg et al. (1996).

We initialise the particle simulation with particles located at every mesh point. The particle positions \mathbf{x}_p are then integrated in time,

$$\mathbf{x}_p = \int_0^t \mathbf{u}_p(\mathbf{x}_p, t') dt'. \quad (13)$$

The gas velocity at those points is obtained via interpolation. We used a second order time step of length $\delta t = 5 \times 10^{-4} T_{\text{rot}}$. In Fig. 1 we show (x, z) -slices of particle positions at six different times for $2\Omega\tau_p = 0.025$, corresponding to a particles size of a little more than 1 cm. Note the rapid concentration of particles into small structures in the meridional plane. These structures are strongly elongated in the azimuthal direction, as can be seen in a fully three-dimensional visualisation (not shown here).

In order to understand the results, let us first look at the quantity $2\boldsymbol{\Omega} \cdot (\boldsymbol{\omega} + \boldsymbol{\Omega})$. Instead of choosing arbitrarily a meridional plane, we consider this quantity averaged in the azimuthal (or y) direction, i.e. $2\Omega(\langle \omega_z \rangle + \Omega)$. It turns out that almost all points have positive values of $2\boldsymbol{\Omega} \cdot (\boldsymbol{\omega} + \boldsymbol{\Omega})$. This suggests that it will be rather hard to accumulate particles anywhere in the box. In Fig. 2 we also show a histogram of ω_z and $\langle \omega_z \rangle$, which shows that the probability of finding a point where the vorticity

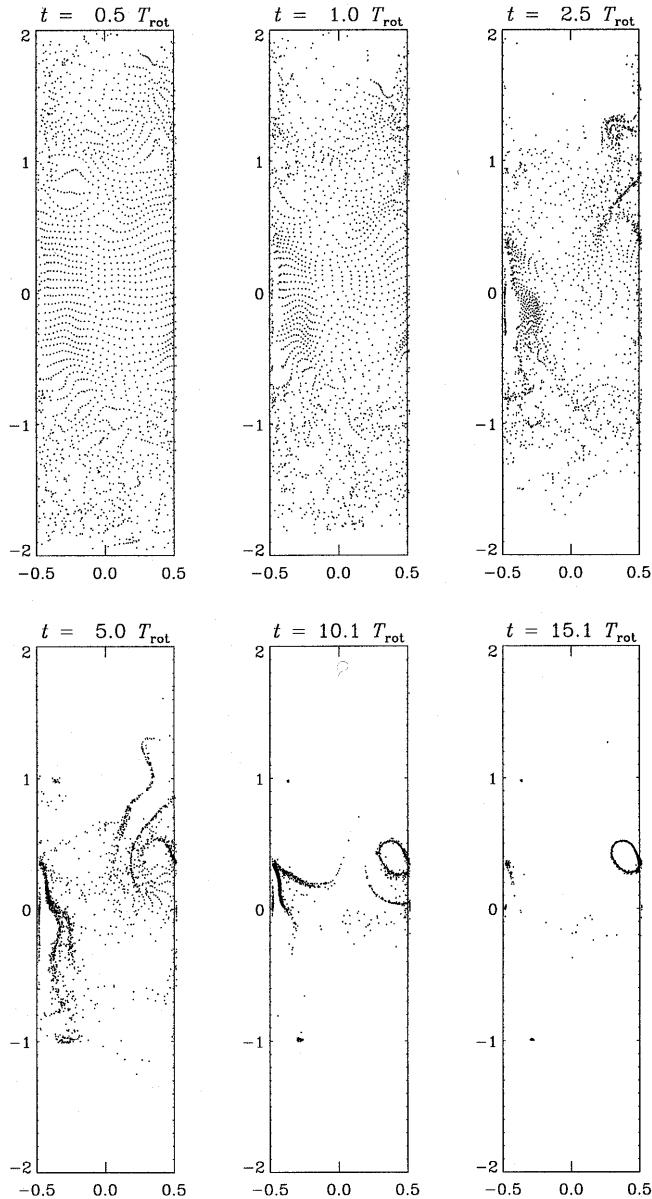


Fig. 1. Meridional slices of particle positions at six different times for $2\Omega\tau_p = 0.025$. The velocity field is frozen in time. Note the rapid formation of structures in the meridional plane and the slow settling of particles in the direction towards the midplane.

is smaller than $-\Omega$ is rather low, even if we do not average in the azimuthal direction.

So, on the one hand our result is disappointing in that the simple minded criterion of particle accumulation in regions with $2\Omega \cdot (\omega + \Omega) < 0$ does not apply. The simulations with frozen velocity field do suggest, however, that particles concentrate regardless of this criterion. This is probably connected with the fact that the gas flow is not solenoidal. Writing down the two-dimensional particle equations, but now in a meridional plane, we can see that the divergence of the particle velocity satisfies

$$(1 + \tau_p \partial_t) (\nabla \cdot \mathbf{u}_p) = -\tau_p \Omega^2 + \nabla \cdot \mathbf{u}. \quad (14)$$

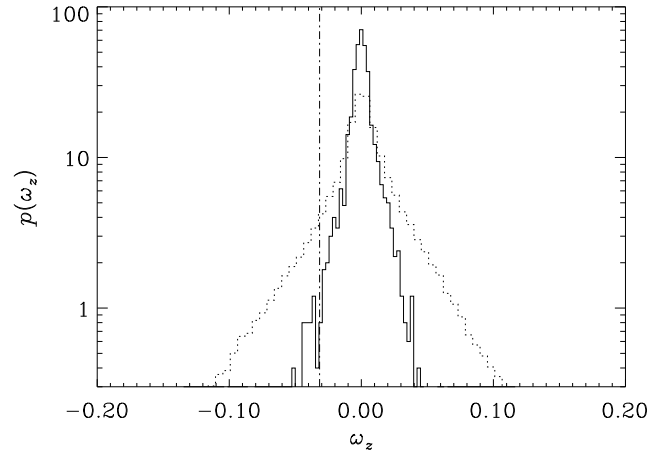


Fig. 2. Histogram of ω_z and $\langle \Omega_z \rangle$. The dashed-dotted vertical line gives the value of $-\Omega$ and shows that the number of points where $\omega_z + \Omega < 0$ is small.

The first term on the right hand side results from the compression of the particle phase due to gravitational settling, and the second term results from the particles simply flowing into points where the gas flow converges. Comparing contour plots of $\nabla \cdot \mathbf{u}$ with Fig. 1 we found that particle accumulation is indeed more common in locations where $\nabla \cdot \mathbf{u} < 0$.

4.2. Evolving velocity field

We now repeat the above calculation using a time evolving velocity field. The simulation has been restarted at $t_0 = 25.3 T_{\text{rot}}$ and Eq. (2) has been solved simultaneously with Eq. (1), as well as the induction equation for the magnetic field, the continuity equation for the gas density ρ and an energy equation for the internal energy. The time step varied in the range $(1 - 5) \times 10^{-4} T_{\text{rot}}$, depending mostly on the instantaneous value of the shock viscosity. For details see Brandenburg et al. (1995a).

Unlike the case of a frozen velocity field there is now no longer a concentration of particles into structures; see Fig. 3. However, the particles still have a tendency to concentrate near the midplane. In Fig. 4 we plot the evolution of the width σ of the particle distribution. The width was calculated from a gaussian fit to a histogram of the particle distribution in the vertical direction. Initially there is a rapid concentration of particles towards the midplane, followed by a slower, approximately exponential, decrease of $\sigma(t)$. For small particles ($2\Omega\tau_p$ around 0.006 or a_p of a few millimeters) the decrease of σ/H tends to level off around $\sigma/H = 1$. When the initial particle distribution is such that $\sigma/H \approx 1$, e.g. case (iv) in Fig. 4, $\sigma(t)$ stays approximately constant. For $\sigma < H$ the turbulence tends to oppose further settling of particles towards the midplane.

We mention in passing that the slight asymmetry about $z = 0$ results from a similar asymmetry in the gas density. This in turn results from stronger turbulence in the lower disc plane at that particular time and may be different at later times.

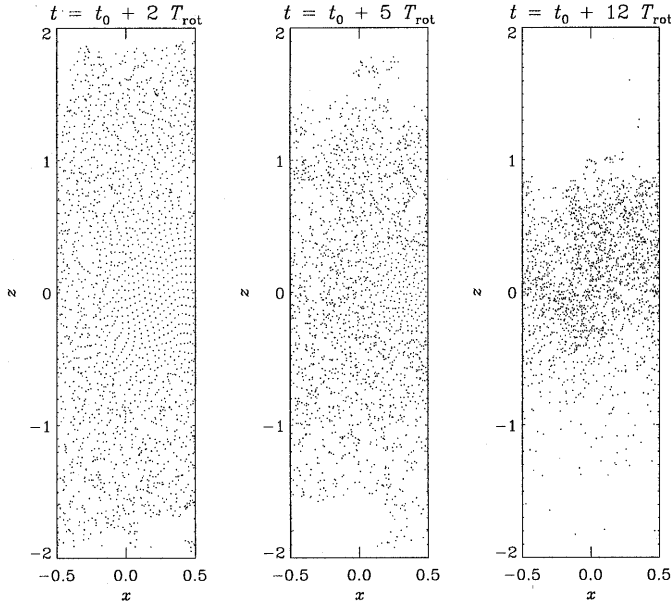


Fig. 3. Meridional slices of particle positions for three different times and $2\Omega\tau_p = 0.025$. Note the absence of particle accumulation into structures and the relatively slow settling of particles in the direction towards the midplane

In order to isolate the effects of gravity from the effects of turbulence we now compare with the case $\mathbf{u} = 0$. In that case the particles move only in the z direction. Eq. (2) reduces then to

$$\ddot{z}_p + \tau_p^{-1} \dot{z}_p + \Omega^2 z_p = 0. \quad (15)$$

Assuming as initial condition $z_p = h$ and $\dot{z}_p = 0$ the solution is

$$z_p(t) = \frac{h}{1 - \Omega^2 \tau_p^2} \left[e^{-\Omega^2 \tau_p t} - \Omega^2 \tau_p^2 e^{-t/\tau_p} \right]. \quad (16)$$

A detailed comparison shows that the evolution of $z_p(t)$ is similar to the evolution of the width σ of the particle distribution during the exponential decay phase (roughly $28 < t/T_{\text{rot}} < 35$; see Fig. 4).

At later times the lighter particles (e.g. $2\Omega\tau_p = 0.006$) begin to deviate from the exponential law of Eq. (16). Lighter particles behave almost like passively advected particles or like a passive scalar. To clarify this point let us briefly consider the evolution equation of the concentration of particles. The number density n_p per unit volume is equal to the density ρ times the concentration c per unit mass, so $n_p = \rho c$, where c is a passive scalar that satisfies an advection-diffusion equation of the form

$$\rho \frac{Dc}{Dt} = \nabla \cdot D \nabla c, \quad (17)$$

where D is a diffusion constant. In a statistically steady state we have $c = \text{const}$. Applied to particles this means that the number density per unit mass is constant, or that the number density n_p per unit volume is proportional to the gas density ρ . In other

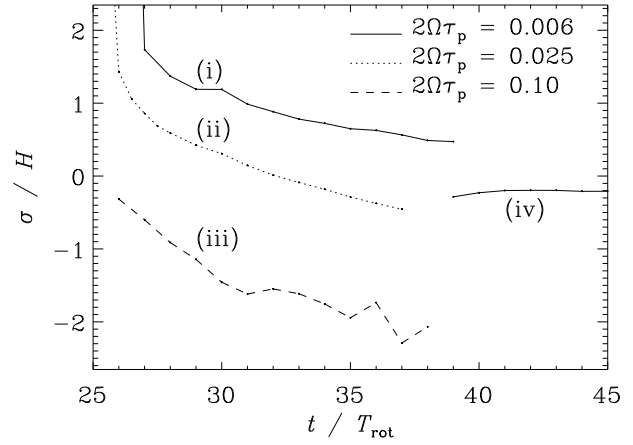


Fig. 4. Evolution of the width $\sigma(t)$ of the particle distribution. (i) and (ii) refer to initially uniformly distributed particles, whereas for (iii) and (iv) the initial particle density is proportional to the gas density ρ

words, the particles tend to approach a state where the vertical dependencies of n_p and n (or σ) are similar. This implies in particular that the scale height of the two distributions is the same, i.e. $\sigma = H$. This is indeed what appears to happen in the simulations. This process may also be responsible for the rapid evolution of particles away from an initial state where the particle density was initially uniform.

Particles approach the state $\sigma = H$ only when $2\Omega\tau_p$ is small enough. From Fig. 4 we estimate that the critical value is somewhere between 0.006 and 0.025, corresponding to a particle size of a few millimeters to one centimeter. This agrees well with the results of Dubrulle et al. (1995), who found that the critical particle size is $a_{\text{crit}} = 150\alpha_{\text{SS}}$ cm, depending on the value of the Shakura-Sunyaev viscosity parameter α_{SS} . In our case $\alpha_{\text{SS}} = 0.005 - 0.01$ (Brandenburg et al. 1996), so $a_{\text{crit}} \approx 1$ cm.

To summarise this section we can say particles that are smaller than a few millimeters are strongly affected by the turbulence which, in turn, leads to a redistribution of particles such that their number density is proportional to the gas density.

5. Charged particles

Micrometer-sized grains are typically charged. This would lead to a current $\mathbf{J}_p = qn_p\mathbf{u}_p$, where q is the charge, and an extra term (the Lorentz force $\mathbf{J}_p \times \mathbf{B}/c$) on the right hand side of Eq. (2),

$$n_p m_p \frac{D\mathbf{u}_p}{Dt} = \dots + \frac{1}{c} q n_p \mathbf{u}_p \times \mathbf{B}, \quad (18)$$

where \mathbf{B} is the magnetic field, c is the speed of light, and gaussian cgs units have been adopted. This additional term causes charged particles to spiral around field lines. The lighter the particle, the tighter the spiral. The importance of this term can be assessed by comparing the gyro frequency of the particle,

$$\omega_p = \frac{qB}{m_p c}, \quad (19)$$

with τ_p^{-1} . For small particles ($a_p \lesssim 10 \mu\text{m}$) the gyro radius is very small compared with H and causes the particles to be closely attached to the magnetic field. For larger particles ω_p decreases and the effect of the gyro term can be neglected.

The magnetic gradient drift could also be important, but it is difficult to assess its effect without detailed calculations, which would go beyond the scope of the present paper. However, it is not obvious that this gradient drift would enhance the settling of particles towards the midplane.

6. Conclusions

Turbulence can strongly affect the settling of dust particles towards the midplane when the particle size is less than only a few millimeters. We find no evidence however that particles accumulate in vortices or anticyclones. Unless the particles are heavy enough, their vertical distribution tends to approach a state where the number density per *unit mass* is approximately constant. Initial tests with a frozen velocity field do unfortunately not provide a useful description of the true dynamics, so it was essential to solve for gas and particle phases simultaneously.

An important piece of physics that is at present not included is coagulation. It would be important to find out whether turbulence could actually enhance the probability of coagulation by more frequent mutual collisions between particles. Another aspect that is presently ignored concerns the dynamics of charged grains. Not only are they affected by the magnetic field, but they also contribute to carrying the current and would in that way feed back onto the dynamics of the gas.

Acknowledgements. We thank Antonello Provenzale for suggesting this kind of work and for helpful discussions in an early stage of the investigations. We also thank Nathan Kleeorin, Igor Rogachevskii and Yuri Sergeev for discussions regarding the 2-fluid approach, Vadim Urpin for pointing out an error in an earlier version of the text, and Berengere Dubrulle for bringing some relevant work to our attention.

References

- Abramowicz, M. A., Lanza, A., Spiegel, E. A., & Szuszkiewicz, E. 1992, *Nat* 356, 41
- Balbus, S. A. & Hawley, J. F. 1991, *ApJ* 376, 214
- Balbus, S. A. & Hawley, J. F. 1992, *ApJ* 400, 610
- Balbus, S. A. & Hawley, J. F. 1996, in *Physics of Accretion Disks*, ed. S. Kato et al (Gordon and Breach Science Publishers), p.279
- Barge, P. & Sommeria, J. 1995, *A&A* 295, L1
- Blaes, O. M., & Balbus, S. A. 1994, *ApJ* 421, 163
- Brandenburg, A., Nordlund, Å., Stein, R. F. & Torkelsson, U. 1995a, *ApJ* 446, 741
- Brandenburg, A., Klapper, I. & Kurths, J. 1995b, *Phys. Rev. E* 52, R4602
- Brandenburg, A., Nordlund, Å., Stein, R. F. & Torkelsson, U. 1996, *ApJ (Letters)* 458, L45
- Cuzzi, J. N., Dobrovolskis, A. R., & Champney, J. M. 1993, *Icarus* 106, 102
- Dubrulle, B. 1993, *Icarus* 106, 59
- Dubrulle, B. & Valdetarro, L. 1992, *A&A* 263, 387
- Dubrulle, B., Morfill, G. & Sterzik, M. 1995, *Icarus* 114, 237
- Elperin, T., Kleeorin, N. & Rogachevskii, I. 1996, *Phys. Rev. Lett.* 76, 224
- Goldreich, P., Ward, W. R. 1973, *ApJ* 183, 1051
- Hawley, J. F., Gammie, C. F., & Balbus, S. A. 1995, *ApJ* 440, 742
- Hawley, J. F., Gammie, C. F., & Balbus, S. A. 1996, *ApJ* 464, 690
- Kley, W., Papaloizou, J. C. B. & Lin, D. N. C. 1993, *ApJ* 416, 679
- Lin, D. N. C. & Papaloizou, J. C. B. 1985, in *Protostars and Planets II*, ed. D. C. Black & M. S. Mathews (University of Arizona Press, Tucson), p.981
- Lynden-Bell, D. & Ostriker, J. P. 1967, *MNRAS* 136, 293
- Matsumoto, R. & Tajima, T. 1995, *ApJ* 445, 767
- Miesch, M., Brandenburg, A., Zweibel, E., & Toomre, J. 1995, in *Proceedings of Fourth SOHO Workshop: Helioseismology*, ed. ESA SP-376, Volume 2 (Pacific Grove, California), p.253
- Regös, E. 1997, *MNRAS* 286, 97
- Reyes-Ruiz, M. & Stepinski, T. F. 1995, *ApJ* 438, 750
- Seinfeld, J. H. 1986, *Atmospheric Chemistry and Physics of Air Pollution* (Wiley, New York)
- Stepinski, T. F., Reyes-Ruiz, M., & Vanhala, H. A. T. 1993, *Icarus* 106, 77
- Stone, J. M., Hawley, J. F., Gammie, C. F., & Balbus, S. A. 1996, *ApJ* 463, 656
- Tanga, P., Babiano, A., Dubrulle, B. & Provenzale, A. 1996, *Icarus* 121, 158
- Weidenschilling, S. J. 1980, *Icarus* 44, 172
- Weidenschilling, S. J. 1984, *Icarus* 60, 553
- Weidenschilling, S. J. & Cuzzi, J. N. 1993, in *Protostars and Planets III*, ed. E. H. Levy, L. J. Lunine & M. S. Mathews (University of Arizona Press, Tucson), p.1031
- Wisdom, J. & Tremaine, S. 1988, *AJ* 95, 925